





RESEARCH ARTICLE

 OPEN ACCESS 

## The pseudokinase MLKL contributes to host defense against *Streptococcus pluranimalium* infection by mediating NLRP3 inflammasome activation and extracellular trap formation

Yu-Xin Lei<sup>a#</sup>, Yang Liu<sup>a,b#</sup>, Li-Hua Xing<sup>a#</sup>, Yu-Jing Wu<sup>a</sup>, Xue-Yin Wang<sup>a</sup>, Fan-Hua Meng<sup>a</sup>, Ya-Nan Lou<sup>a</sup>, Zhao-Guo Ma<sup>a</sup>, Lin Yuan <sup>a,c</sup>, and Shui-Xing Yu <sup>a,c</sup>

<sup>a</sup>State Key Laboratory of Reproductive Regulation and Breeding of Grassland Livestock, College of Life Sciences, Inner Mongolia University, Hohhot, China; <sup>b</sup>Animal Husbandry Institute, Agriculture and Animal Husbandry Academy of Inner Mongolia, Hohhot, China; <sup>c</sup>Inner Mongolia Engineering Technology Research Center of Germplasm Resources Conservation and Utilization, College of Life Sciences, Inner Mongolia University, Hohhot, China

### ABSTRACT

Host innate immunity plays a pivotal role in the early detection and neutralization of invading pathogens. Here, we show that pseudokinase mixed lineage kinase-like protein (MLKL) is required for host defence against *Streptococcus pluranimalium* infection by enhancing NLRP3 inflammasome activation and extracellular trap formation. Notably, *Mkl1* deficiency leads to increased mortality, increased bacterial colonization, severe destruction of organ architecture, and elevated inflammatory cell infiltration in murine models of *S. pluranimalium* pulmonary and systemic infection. *In vivo* and *in vitro* data provided evidence that potassium efflux-dependent NLRP3 inflammasome signalling downstream of active MLKL confers host protection against *S. pluranimalium* infection and initiates bacterial killing and clearance. Moreover, *Mkl1* deficiency results in defects in extracellular trap-mediated bactericidal activity. In summary, this study revealed that MLKL mediates the host defence response to *S. pluranimalium*, and suggests that MLKL is a potential drug target for preventing and controlling pathogen infection.

### ARTICLE HISTORY

Received 18 April 2023  
Revised 27 August 2023  
Accepted 29 August 2023

### KEYWORDS

*S. pluranimalium*; innate immunity; mixed lineage kinase-like protein; NLRP3 inflammasome; extracellular trap

## Introduction


*Streptococcus pluranimalium*, a new species of streptococci, was first isolated from diseased livestock in 1999 [1]. *S. pluranimalium* persistently colonize the genital tract, udder and tonsils of mammals, and crop, skin and respiratory tract of birds, presented an indication of the possible existence within *S. pluranimalium* of typical host-specific or even site-specific characteristics [1]. In recent years, *S. pluranimalium* has been regarded as a pathogen associated with meningoencephalitis in a horse [2], valvular endocarditis and septicaemia in adult broiler parents [3], bovine mastitis and bovine reproductive disease [4,5]. Meanwhile, Aryasinghe L et al. reported the first case of a subdural empyema caused by *S. pluranimalium*, in a healthy adolescent male as a possible complication of subclinical frontal sinusitis [6]. Factually, *S. pluranimalium* also has been reported to cause infective endocarditis, brain abscess and pneumonia with synpneumonic effusion and bacteraemia in a healthy adult [7–9]. These indicate *S. pluranimalium*

may be a novel human pathogen. Although there is growing scientific concern over antibiotic resistance, cephalosporins, aminoglycosides, vancomycin, and linezolid are currently the recommended first-line treatments for *S. pluranimalium* infection [10]. Therefore, it is necessary for development of novel therapeutic strategies to combat *S. pluranimalium* infections.

The innate immune system is the first line of host defence against pathogens invasion. Sensing non-self and endogenous danger signals from microbial infection or tissue injury, known as pathogen-associated molecular patterns (PAMPs) and damage-associated molecular patterns (DAMPs) [11,12] through interaction with pattern recognition receptors (PRRs). The host innate immune cells are equipped with an arsenal of PRRs to identify microbial invaders and direct effective immune responses that initiate defence mechanisms. Several families of PRRs, including NOD-like receptors (NLRs) [13], cytosolic DNA receptors [14], Toll-like receptors (TLRs) [15], RIG-I-like receptors

**CONTACT** Lin Yuan  [yuanlin@imu.edu.cn](mailto:yuanlin@imu.edu.cn); Shui-Xing Yu  [shuixingyu@imu.edu.cn](mailto:shuixingyu@imu.edu.cn)

<sup>#</sup>These authors contributed equally to this work.

 Supplemental data for this article can be accessed online at <https://doi.org/10.1080/21505594.2023.2258057>

© 2023 The Author(s). Published by Informa UK Limited, trading as Taylor & Francis Group.

This is an Open Access article distributed under the terms of the Creative Commons Attribution-NonCommercial License (<http://creativecommons.org/licenses/by-nc/4.0/>), which permits unrestricted non-commercial use, distribution, and reproduction in any medium, provided the original work is properly cited. The terms on which this article has been published allow the posting of the Accepted Manuscript in a repository by the author(s) or with their consent.

(RLRs) [16] and C-type lectin receptors [17] are implicated in recognizing invading microbes and preventing infectious diseases. *S. pluranimalium*, a serious pathogen that poses a threat to public and animal health. Therefore, it is not surprising that investigating the innate immune mechanisms of host resistance to *S. pluranimalium* is conducive to the development of effective strategies for controlling this infection.

The pseudokinase mixed lineage kinase-like protein (MLKL) is considered a canonical necroptotic executor protein and was initially discovered by Sun et al. [18]. It functions as a downstream target of the receptor interacting protein kinase (RIPK) 1 and RIPK3 [19,20]. When MLKL is activated, including MLKL phosphorylation, oligomerization, and membrane translocation, pores are eventually formed to directly execute a necrotic form of cell death, termed necroptosis [21,22]. Increasing evidence has revealed that active MLKL-mediated necroptosis confers host protection against pathogen infections [23,24] and is associated with numerous inflammatory diseases [25–27]. To date, the overwhelming majority of the current research on active MLKL has focused on its role in cell death, and the prevalent idea has been that the sole responsibility of active MLKL is to initiate necroptosis. Several studies, including ours, indicate that active MLKL can serve as a modulator of various diseases via its non-necroptotic activities [25,28,29]. Actually, biological functions of active MLKL functions beyond serving as the executioner of necroptosis, including regulation of gene expression, interaction with other regulated cell death (RCD) pathways, and binding to select lipids to block specific processes [30]. Although these novel roles of active MLKL highlight its conserved functional complexity and diversity, the biological implications of active MLKL in innate immunity during pathogen invasion remain poorly understood.

In this study, we revealed the beneficial role of MLKL in the host defence against *S. pluranimalium* infection. *Mlkl*<sup>-/-</sup> (*Mlkl*-deficient) mice are more susceptible to *S. pluranimalium* infection compared with WT (wild-type) counterparts, with increased bacterial loads, higher survival rates, and severe organ damage. Most importantly, the protective effect of MLKL against *S. pluranimalium* infection is dependent on its ability to potentially promote bacterial killing and clearance processes. Potassium efflux-dependent NLRP3 inflammasome signalling downstream of MLKL facilitates bacterial eradication. Interestingly, the formation of extracellular trap also participates in the MLKL-elicited

bactericidal activity. Collectively, our results suggested that MLKL is essential for host defence against *S. pluranimalium* infection by enhancing NLRP3 inflammasome activation and extracellular trap formation.

## Materials and methods

### Mice and cells

*Mlkl*<sup>-/-</sup> mice were kindly provided by Dr. Jia-Huai Han of Xiamen University, China. *Nlrp3*<sup>-/-</sup> and C57BL/6J (WT) mice were purchased from Jackson Laboratory (Bar Harbor, ME, USA). They were subsequently backcrossed onto a C57BL/6J background for at least eight generations. Age- and sex-matched WT controls were included in this study. All the mice were maintained in a pathogen-free environment at the Laboratory Animal Center of Inner Mongolia University. All experiments were conducted according to experimental practices and standards approved by the Animal Welfare and Research Ethics Committee of Inner Mongolia University ([2020]022). Bone marrow-derived macrophages (BMDMs) were prepared and isolated from femurs of 6–8 weeks old mice, and cultured in RPMI1640 medium (Gibco, #31800–022) containing 10% foetal bovine serum (FBS, Gibco, #A31608–02), 25% L929 cell – conditioned medium, and 100 U/mL penicillin/streptomycin (P/S, Gibco, #15140–122) at 37°C in a humidified atmosphere containing 5% CO<sub>2</sub>. Mature cells were harvested for assays on day 7 of differentiation.

### Bacterial culture and animal infection

*S. pluranimalium* strain STP1, a clinical isolate of *S. pluranimalium* (16S rDNA sequencing analysis (Figures S1A, B), and specific 16S rDNA gene sequence data deposited in NCBI GenBank: OQ073875) was isolated from nasal swab samples in ovine with signs of respiratory tract disease and was grown at 37°C in tryptic soy broth (TSB) medium. Six-to eight-week-old sex-matched mice were intranasally or *i.v.* inoculated with  $1 \times 10^9$  or  $1 \times 10^8$  colony-forming units (CFUs) log-phase *S. pluranimalium* strain STP1 diluted in PBS in a total volume of 50 or 100  $\mu$ L. For the administration of exogenous recombinant IL-1 $\beta$  (rIL-1 $\beta$ ), mice were intranasally administered PBS alone (control) or with rIL-1 $\beta$  (Novoprotein, #C042) at a dose of 1.0  $\mu$ g per mouse in 100  $\mu$ L PBS on day-1 and day 0. The mice were infected with *S. pluranimalium* strain STP1 on day 0.

### **Bacterial loads and cytokine release measurements**

Aseptically bronchoalveolar lavage fluid (BALF) and excised tissue homogenates (homogenized mechanically in cold PBS at a ratio of 4 mL per gram tissue) were collected at 24 hpi., serially diluted and plated onto TSB agar plates for bacterial enumeration (CFUs/g). To measure the levels of cytokines and chemokines, the tissues were homogenized mechanically in cold PBS (at a ratio of 4 g tissue/mL) containing a complete protease inhibitor cocktail (Sigma-Aldrich, #9036-19-5) and 1% Triton X-100 (Sigma-Aldrich, #93443). Cytokines and chemokines in lung tissue homogenates or cell culture supernatants were determined by ELISA (R&D Systems) according to the manufacturer's instructions.

### **Inflammasome activation assay**

BMDMs were pre-treated with 500 ng/mL LPS (Invitrogen, #tlrl-3pelps) for 4 h and then washed twice with serum-free RPMI-1640 medium. LPS-primed BMDMs were incubated with or without 50 mM potassium chloride (Sigma-Aldrich, #1049360250) for 30 min before stimulation with ATP (5 mM, 30 min, Sigma, #A2383) or *S. pluranimalium* strain STP1 (MOI = 50, 5 h). Subsequently, cell supernatants and cell extracts were collected for ELISA and immunoblotting analyses.

### **Histopathology and immunostaining analysis**

The excised lung and kidney tissues were fixed immediately with 4% PFA (#P804536; Macklin) for histological and immunostaining analyses. Sections (5 µm thick) were prepared from paraffin-embedded tissues and subjected to haematoxylin and eosin (H&E, Solarbio, #SL7050-500) staining. Immunostaining was performed using anti-Ly-6 G/Ly-6c (1:100, BioLegend, #108419), anti-F4/80 (1:100; BioLegend, #123119), anti-p-MLKL (1:100; Abcam, #ab196436), and anti-histone (1:100, ABclonal, #A2348) antibodies. The presence of death cells in lung and kidney sections was determined using terminal deoxynucleotide transferase dUTP nick end-labelling (TUNEL) staining kit (KeyGEN BioTECH, #KGA7061) following the manufacturer's manual.

### **METs formation assay**

The matured BMDMs were plated onto poly L-lysine-coated coverslips, and incubated with LPS (500 ng/mL, 4 h, Invitrogen, #tlrl-3pelps) before being stimulated

with *S. pluranimalium* strain STP1 (MOI = 25, 100 min). The macrophage extracellular traps (METs) were determined using anti-histone (1:100, ABclonal, #A2348), anti-MPO (1:100, Biorbyt, #orb16003), SYTOX Orange`1 (5 mM, Invitrogen, #S-11368), Hoechst 33,342 (2 mM, Wanleibio, #WLA042a), and Alexa Fluor®488-conjugated anti-rabbit IgG antibodies. Images were acquired and analysed using a Laser Co-focus light microscope (Nikon). For scanning electron microscopy (SEM) analysis, the samples were sputtered with gold and then measured by SEM according to the manufacturer's instructions (Servicebio Technology Co., LTD, Wuhan, China). To quantify METs formation, the extracellular DNA content in the supernatants was determined using SYTOX Green (5 mM, Invitrogen, #S7020) using a Varioskan Flash plate reader (Thermo Scientific). Cells treated with zymosan (1 mg/ml) served as positive controls.

### **Bacterial killing assay**

To determine the bacterial killing capacity of macrophages, LPS-primed BMDMs were incubated with or without rIL-1β (1000 pg/mL, 1 h) before inoculation with *S. pluranimalium* strain STP1 (MOI = 25, 6 h). The cell supernatants were collected and plated on TSB agar plates to enumerate the bacteria after overnight culture.

### **Protein extraction and immunoblotting analysis**

The tissues or BMDMs were lysed in an ice-cold lysis buffer containing 1% Triton X-100 (Sigma-Aldrich, #93443), 50 mM Tris-HCl (pH 7.4, Sigma-Aldrich, #10812846001), 150 mM NaCl (Sigma-Aldrich, #S3014), 0.1 mM Na<sub>3</sub>VO<sub>4</sub> (Sigma-Aldrich, #S6508) and complete protease inhibitor cocktail (Sigma-Aldrich, #P8340). The supernatants (Sup.) of cells were collected and precipitated using methanol-chloroform extraction to obtain the cell lysate. Tissues and cell extracts were separated by SDS-PAGE and transferred to a polyvinylidene fluoride (PVDF) membrane. The membranes were incubated with anti-Caspase-1 (1:1000, Adipogen, #A28881708) and IL-1β (1:1000, Adipogen, #PRP1119). Equal loading was confirmed by probing with GADPH (1:2000, Proteintech, #60004-1-Ig).

### **Statistical analysis**

Data are presented as the mean ± standard deviation (SD). Differences between the mean values of normally distributed data were analysed using one-way ANOVA

(Dunnett's t-test) and two-tailed Student's t-test. The log-rank test was used for statistical analysis of animal mortality. \* $p < 0.05$  and \*\* $p < 0.01$  compared with control group. Statistical analyses were performed using Prism software (GraphPad Software, La Jolla, CA, USA).

## Results

### ***Mkl* deficiency attenuates bacterial clearance during *S. pluranimalium* pulmonary infection**

To explore the possible involvement of MLKL in the host response to *S. pluranimalium* infection *in vivo*, a murine *S. pluranimalium* pneumonia model was successfully established. WT (wild-type) and *Mkl*<sup>-/-</sup> (*Mkl*-deficient) mice (per mouse) were intranasally challenged with  $1 \times 10^9$  colony-forming units (CFUs) of log-phase *S. pluranimalium* strain STP1, a clinical isolate of *S. pluranimalium* (16S rDNA sequencing analysis (Figures S1A, B), and specific 16S rDNA gene sequence data deposited in NCBI GenBank: OQ073875). At 24 h post-infection (hpi), bacterial loads were detected in the lung and bronchoalveolar lavage fluid (BALF) by CFUs counting. Elevated levels of bacteria were observed in the lung tissues and BALF of *Mkl*<sup>-/-</sup> mice compared to WT mice (Figures 1a,b), which was similar to previous reports that *Mkl*<sup>-/-</sup> mice harboured increased loads of *Streptococcus pneumoniae* in the lungs [31,32]. In accordance with the high bacterial burden, pathological evaluation of the extent of protein content in BALF (Figure 1c), epithelial cell damage, inflammatory cell infiltration, and expression of chemokine KC revealed that *Mkl*<sup>-/-</sup> mice displayed markedly severe pulmonary damage and exacerbated distortion of the lung architecture (Figures 1(d-h)), suggesting that *Mkl*<sup>-/-</sup> mice were more susceptible to *S. pluranimalium* infection. Subsequently, to further substantiate the protective role of MLKL in the host defence against *S. pluranimalium*, the experiment was repeated with the intranasal administration of log-phase *S. pluranimalium* and the mortality of mice was monitored. Compared with their WT counterparts, *Mkl*<sup>-/-</sup> mice showed a slight trend towards decreased survival, but no differences between them were noted (Figure 1i). Accordantly, Huang H-R *et al.* found that *Mkl* deficiency leads to excessive inflammation and severe histological damage during *S. pneumoniae* pulmonary infection [32]. Together, these suggest that MLKL may play an indispensable role in the lungs and contribute to host protection against *S. pluranimalium* pneumonia.

### ***Mkl* deficiency results in the defect of bacterial clearance following *S. pluranimalium* systemic infection**

Given that MLKL is involved in host defence against *S. pluranimalium* pulmonary infection, we set out to determine whether MLKL also regulates host protection against *S. pluranimalium* systemic infection. WT and *Mkl*<sup>-/-</sup> mice (per mouse) were intravenously infected with  $1 \times 10^8$  CFUs of log-phase *S. pluranimalium*. The effect of MLKL on the bacterial burden was assessed at 24 hpi. As expected, *Mkl*<sup>-/-</sup> mice showed significantly increased bacterial loads in the blood, kidney, liver, and spleen compared with WT mice (Figures 2(a-d)), indicating that *Mkl* deficiency facilitates bacterial growth and dissemination. Consistent with this, *Mkl*<sup>-/-</sup> mice displayed more severe kidney injury than WT mice, as demonstrated by haematoxylin and eosin (H&E) histology and TUNEL staining (Figures 2(e,f)). Massive macrophage and neutrophil accumulation in the kidney were also elevated in *Mkl*<sup>-/-</sup> mice following *S. pluranimalium* challenge (Figures 2(g,h)). Thus, these results suggest that MLKL is involved in the host defence against *S. pluranimalium* systemic infection.

### **MLKL-driven inflammasome activation prevents bacterial colonization**

To investigate the potential mechanisms that contribute to higher bacterial burdens in *Mkl*<sup>-/-</sup> mice, we first evaluated inflammasome signalling, because inflammasome activation is essential for host innate immune defence against pathogenic infection. Strikingly, our results revealed that Caspase-1 cleavage, a common event associated with inflammasome activation, was strongly decreased in the lungs of infected *Mkl*<sup>-/-</sup> mice relative to the levels observed in infected WT mice following *S. pluranimalium* infection (Figure 3a). In particular, the production of inflammasome dependent IL-1 $\beta$  was also significantly inhibited in the lung tissues of *Mkl*<sup>-/-</sup> mice compared to that in WT mice (Figures 3a,b). In contrast, TNF- $\alpha$  secretion did not appear to be markedly different between mice of both genotypes (Figure 3c). These data suggest that *Mkl* deficiency potently suppresses inflammasome activation during *S. pluranimalium* infection. Subsequently, to further determine whether inflammasome signalling downstream of MLKL confers host protection against *S. pluranimalium* infection, *Mkl*<sup>-/-</sup> mice were administered exogenous recombinant IL-1 $\beta$  (rIL-1 $\beta$ ) and whether exogenous rIL-1 $\beta$  treatment could rescue the susceptibility to infection in *Mkl*<sup>-/-</sup> mice was evaluated. Notably, exogenous rIL-1 $\beta$  administration resulted in



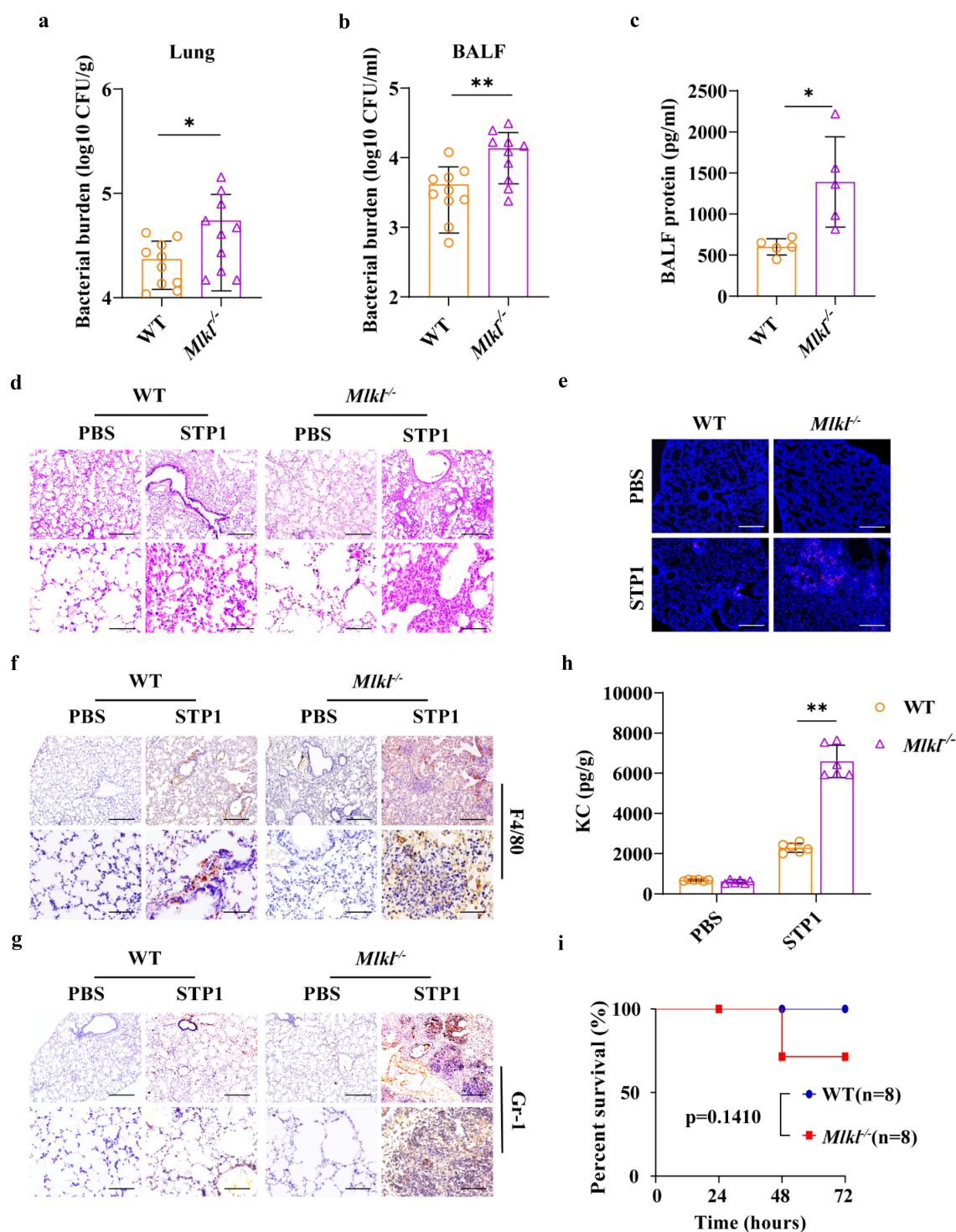


**Figure 1.** *Mik1*<sup>-/-</sup> mice display increased susceptibility to *S. pluranimalium* pulmonary infection. Age- and sex-matched WT and *Mik1*<sup>-/-</sup> mice ( $n = 10$ ) were infected intranasally with  $1 \times 10^9$  CFUs *S. pluranimalium* strain STP1. (A, B) bacterial loads in the lung and BALF were determined at 24 h p.i. (C) total protein in BALF was assessed. (D) representative lung tissue structures were observed by H&E staining (upper panel, magnification  $\times 100$ , lower panel, magnification,  $\times 400$ ). (E) representative TUNEL staining of apoptotic cells in the lung tissue (magnification,  $\times 400$ ). (F, G) representative immunohistochemical staining of F4/80 (a macrophages marker) and gr-1 (a neutrophil marker) were detected in lung sections (upper panel, magnification  $\times 100$ , lower panel, magnification,  $\times 400$ ). (H) level of KC in lung homogenate supernatant was determined. (I) survival was monitored up to 72 h p.i. ( $n = 8$  each group). Graphs are means  $\pm$  standard deviation (SD) from data pooled 10 (A and B), five (C) or six (H) biological replicates. Statistical significance is indicated by \* $p < 0.05$ , \*\* $p < 0.01$ .

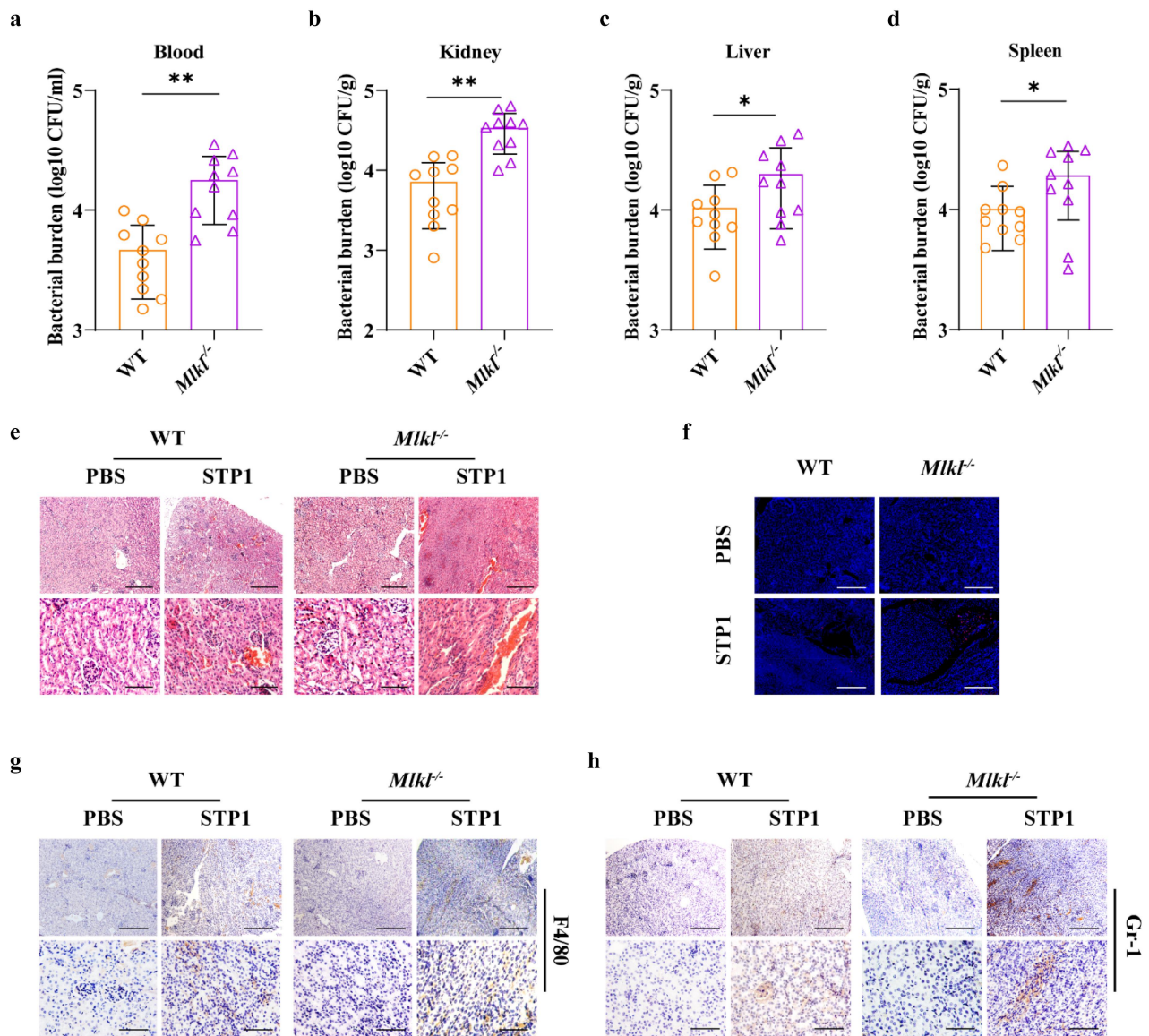


**Figure 2.** *Mik1*<sup>-/-</sup> mice display increased susceptibility to *S. pluranimalium* systemic infection. Age- and sex-matched WT and *Mik1*<sup>-/-</sup> mice ( $n = 10$ ) were infected *i.v.* with  $1 \times 10^8$  CFUs *S. pluranimalium* strain STP1. (A-D) bacterial burden in blood, kidney, liver and spleen were quantitated at 24 hpi. (E) representative kidney tissue structures were observed by H&E staining (upper panel, magnification  $\times 100$ , lower panel, magnification,  $\times 400$ ). (F) representative TUNEL staining of apoptotic cells in the kidney tissue (magnification,  $\times 400$ ). (G, H) representative immunohistochemical staining of F4/80 (a macrophages marker) and gr-1 (a neutrophil marker) were detected in kidney sections (upper panel, magnification  $\times 100$ , lower panel, magnification,  $\times 400$ ). Graphs are means  $\pm$  SD from data pooled 10 (A-D) biological replicates. Statistical significance is indicated by \* $p < 0.05$ , \*\* $p < 0.01$ .

a reduced bacterial load in the lungs, BALF, blood, and kidney of *Mik1*<sup>-/-</sup> mice, which was comparable to that observed in WT mice, suggesting that inflammasome inhibition is detrimental to bacterial control in *Mik1*<sup>-/-</sup> mice following *S. pluranimalium* infection (Figures 3(d-g)). Moreover, exogenous rIL-1 $\beta$  administration significantly alleviated pathological damage in the lungs and kidneys of *Mik1*<sup>-/-</sup> mice (Figures 3(h-i)). Collectively, these results indicate that MLKL facilitates pathogen control in an inflammasome-dependent manner.

### **NLRP3 inflammasome signalling downstream of MLKL mediates host defence**

To characterize the signalling mechanisms underlying MLKL-mediated host defence, the expression of phosphorylated MLKL (p-MLKL) in lung and kidney sections was examined by immunohistochemical staining. Our results revealed that p-MLKL was mainly located in the recruited inflammatory cells of the infected lungs and kidneys (Figures 4a,b). Subsequently, we set out to illustrate the immune response upon infection with the

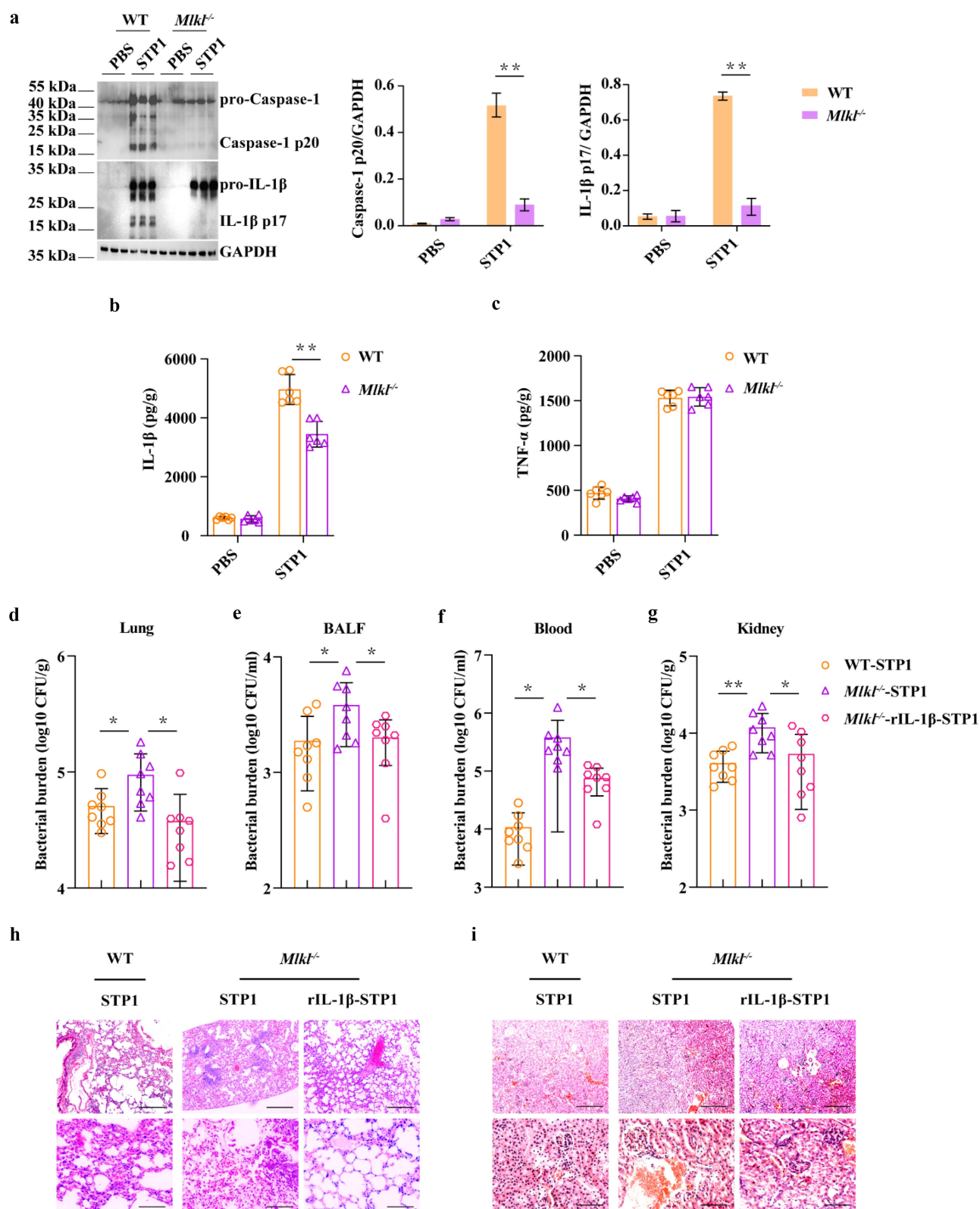


**Figure 3.** Inflammasome signalling is required for MLKL-mediated host protection against *S. pluranimalium* infection. Age- and sex-matched WT and *Mik1<sup>-/-</sup>* mice were infected intranasally with log-phase *S. pluranimalium* strain STP1 ( $1 \times 10^9$  CFUs) for 24 h. (A) lung tissues were collected, homogenized, and then immunoblotting for Caspase-1, IL-1 $\beta$  and GAPDH. Left, representative immunoblotting for Caspase-1 and IL-1 $\beta$  in lung tissues. Right, amounts of Caspase-1 and IL-1 $\beta$  determined by densitometry of protein bands from three experiments. The GAPDH served as a loading control. (B, C) levels of IL-1 $\beta$  and TNF- $\alpha$  in lung were determined. For one group of *Mik1<sup>-/-</sup>* mice, 1.0  $\mu$ g exogenous rIL-1 $\beta$  was injected intraperitoneally daily starting the day prior to the intranasally ( $1 \times 10^9$  CFUs) or *i.v.* ( $1 \times 10^8$  CFUs) inoculated with *S. pluranimalium* strain STP1 ( $n = 8$  each group, at 24 h p.i.). (D-G) bacterial loads in the lung, BALF, blood and kidney were determined. (H, I) representative lung and kidney tissue structures were observed by H&E staining (upper panel, magnification  $\times 100$ , lower panel, magnification,  $\times 400$ ). Graphs are means  $\pm$  SD from data pooled six (B-C) or eight (D-G) biological replicates. Statistical significance is indicated by  $*p < 0.05$ ,  $**p < 0.01$ .



pathogen *S. pluranimalium* in macrophages *in vitro* because these cells are essential for pathogen clearance. In line with this, p-MLKL protein levels were markedly up-regulated by bacterial challenge in the infected WT bone marrow-derived macrophages (BMDMs) and absent in *Mkl1*<sup>-/-</sup> BMDMs (Figure 4c). Since active MLKL triggers the NLRP3 inflammasome in a cell-intrinsic manner, providing a mechanism for the concurrent processing and release of IL-1β [33,34]. Next, we investigated whether *Mkl1* deficiency impairs inflammasome signalling in macrophages. Consistent with *in vivo* results, inflammasome signalling was markedly inhibited in *Mkl1*<sup>-/-</sup> BMDMs vs. WT BMDMs following log-phase *S. pluranimalium* challenge, as demonstrated by impaired Caspase-1 and IL-1β cleavages, and reduced mature IL-1β secretion (Figures 4d-f). To further dissect this pathway, we analysed whether MLKL-driven inflammasome activation was dependent on NLRP3 signalling. In accordance with *Mkl1*<sup>-/-</sup> BMDMs, inflammasome signalling was significantly suppressed in *Nlrp3*<sup>-/-</sup> macrophages, as revealed by impaired Caspase-1 and IL-1β cleavage (Figure 4g) and decreased mature IL-1β secretion (Figure 4h), although TNF-α production was not affected (Figure 4i). In particular, *S. pluranimalium*-triggered NLRP3 inflammasome signalling was found to be inhibited by increasing the extracellular potassium concentrations, as shown by impaired Caspase-1 and IL-1β cleavage (Figure 4j), and reduced mature IL-1β secretion (Figure 4k), whereas TNF-α production did not appear to be obviously different (Figures 4 l), indicating that *S. pluranimalium* triggered NLRP3 inflammasome activation in a potassium efflux-dependent manner. In conclusion, these data provide *in vitro* evidence that *Mkl1* deficiency generates weaker and delayed NLRP3 inflammasome responses relative to *S. pluranimalium* infection.

To further substantiate whether NLRP3 inflammasome signalling mediates MLKL's effect of MLKL on host defence, *Nlrp3*<sup>-/-</sup> mice were used to assess the role of NLRP3 in pulmonary and systemic host defence against *S. pluranimalium* infection. A similar defect in host defence was observed in *Nlrp3*<sup>-/-</sup> mice, as demonstrated by significantly increased bacterial loads in the lungs, BALF, blood, kidneys, livers, and spleens (Figures 5(a-f)), severe lung and kidney injury (Figures 5(g-j)), and impaired inflammasome activation (Figures 5(k-m)), which are consistent with findings in *Mkl1*<sup>-/-</sup> mice. Furthermore, exogenous rIL-1β treatment

reduced the bacterial burden (Figures S2A-E) and alleviated pathological damage (Figures S2F and G) in *Mkl1*<sup>+/-</sup>/*Nlrp3*<sup>+/-</sup> mice during *S. pluranimalium* infection. In particular, *Mkl1*<sup>-/-</sup> and *Nlrp3*<sup>-/-</sup> BMDMs were incapable of killing bacteria compared to WT BMDMs, whereas exogenous rIL-1β treatment could rescue the bacterial killing defect in *Mkl1*<sup>-/-</sup> and *Nlrp3*<sup>-/-</sup> BMDMs (Figures 5n, o). In conclusion, these results revealed that NLRP3 inflammasome signalling is implicated in active MLKL-mediated host defence against *S. pluranimalium* infection.

### ***Mkl1* deficiency leads to a reduction of extracellular trap formation**

Because of the defect in pathogen control in the absence of *Mkl1*, we next investigated whether other mechanisms also account for MLKL-mediated bactericidal activity. Recently, the formation of extracellular traps (ETs) has been proposed as a novel bactericidal mechanism in several types of innate immune cells. To assess the functional role of MLKL in ETs formation, WT and *Mkl1*<sup>-/-</sup> BMDMs were subjected to immunofluorescence co-staining for DNA, histone, and MPO, core components of ETs. The formation of macrophage extracellular traps (METs) was significantly reduced in *Mkl1*<sup>-/-</sup> BMDMs compared to that in WT BMDMs (Figures 6a,b). To quantify METs release, the extracellular DNA content was measured in the supernatants. *Mkl1*<sup>-/-</sup> BMDMs showed a similar trend, with a markedly decreased extracellular DNA content (Figure 6c). Scanning electron microscopy (SEM) analysis revealed that the exposure of WT BMDMs to *S. pluranimalium* resulted in the formation of a delicate network of thicker and thinner strands of fibres originating from cells and firmly attached to the bacterial surface, seemingly entrapping them. However, this effect was weakened in *Mkl1*<sup>-/-</sup> BMDMs during *S. pluranimalium* challenge (Figure 6d). Likewise, a reduction in histone expression was observed in the lung and kidney tissues of infected *Mkl1*<sup>-/-</sup> mice compared to those of infected WT mice (Figures 6e,f). Altogether, these data suggest that the protective effect of MLKL against *S. pluranimalium* infection may also depend on ETs-mediated pathogen control.

### **Discussion**

*S. pluranimalium* infections have been proved to pose a potential threat to public health and the animal industry, and science shows that they can be transmitted via the respiratory tract, mucosa, digestive tract, and skin



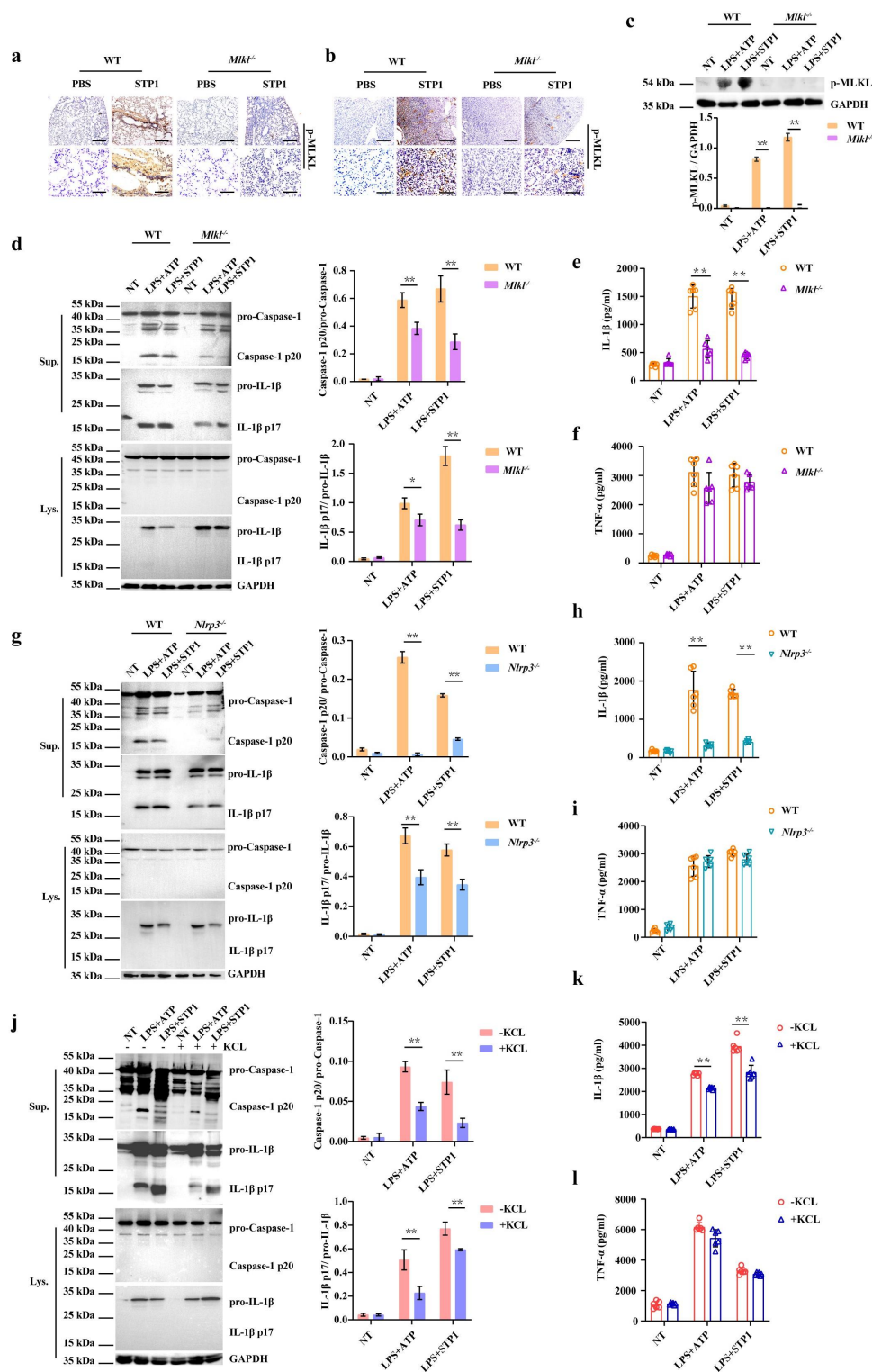


**Figure 4.** *Mkl1* deficiency suppresses NLRP3 inflammasome signalling. Age- and sex-matched WT and *Mkl1*<sup>-/-</sup> mice were infected intranasally ( $1 \times 10^9$  CFUs) or *i.v.* ( $1 \times 10^8$  CFUs) with *S. pluranimalium* strain STP1 for 24 h. (A, B) representative immunohistochemical staining of p-MLKL was performed in lung and kidney sections (upper panel, magnification  $\times 100$ , lower panel, magnification,  $\times 400$ ). LPS-primed WT, *Mkl1*<sup>-/-</sup> and *Nlrp3*<sup>-/-</sup> BMDMs were incubated with or without potassium chloride for 30 min, followed by treatment with ATP (5 mM, 30 min) or *S. pluranimalium* strain STP1 (MOI = 50, 5 h). (C) top, representative images of immunoblotting for p-MLKL in cell lysates. Bottom, amounts of p-MLKL were quantified from three experiments. The GAPDH served as a loading control. (D, G and J) Left, representative immunoblotting for Caspase-1 and IL-1 $\beta$  in cell supernatants and cell extracts. The GAPDH served as a loading control. Right, amounts of Caspase-1 and IL-1 $\beta$  determined by densitometry of protein bands from three experiments. The cells with no treatment (NT) were taken as the control group. (E, F, H, I, K and L) culture supernatants were analysed for IL-1 $\beta$  and TNF- $\alpha$  by ELISA. Graphs are means  $\pm$  SD from data pooled six (E, F, H, I, K and L) biological replicates. Statistical significance is indicated by \* $p < 0.05$ , \*\* $p < 0.01$ .

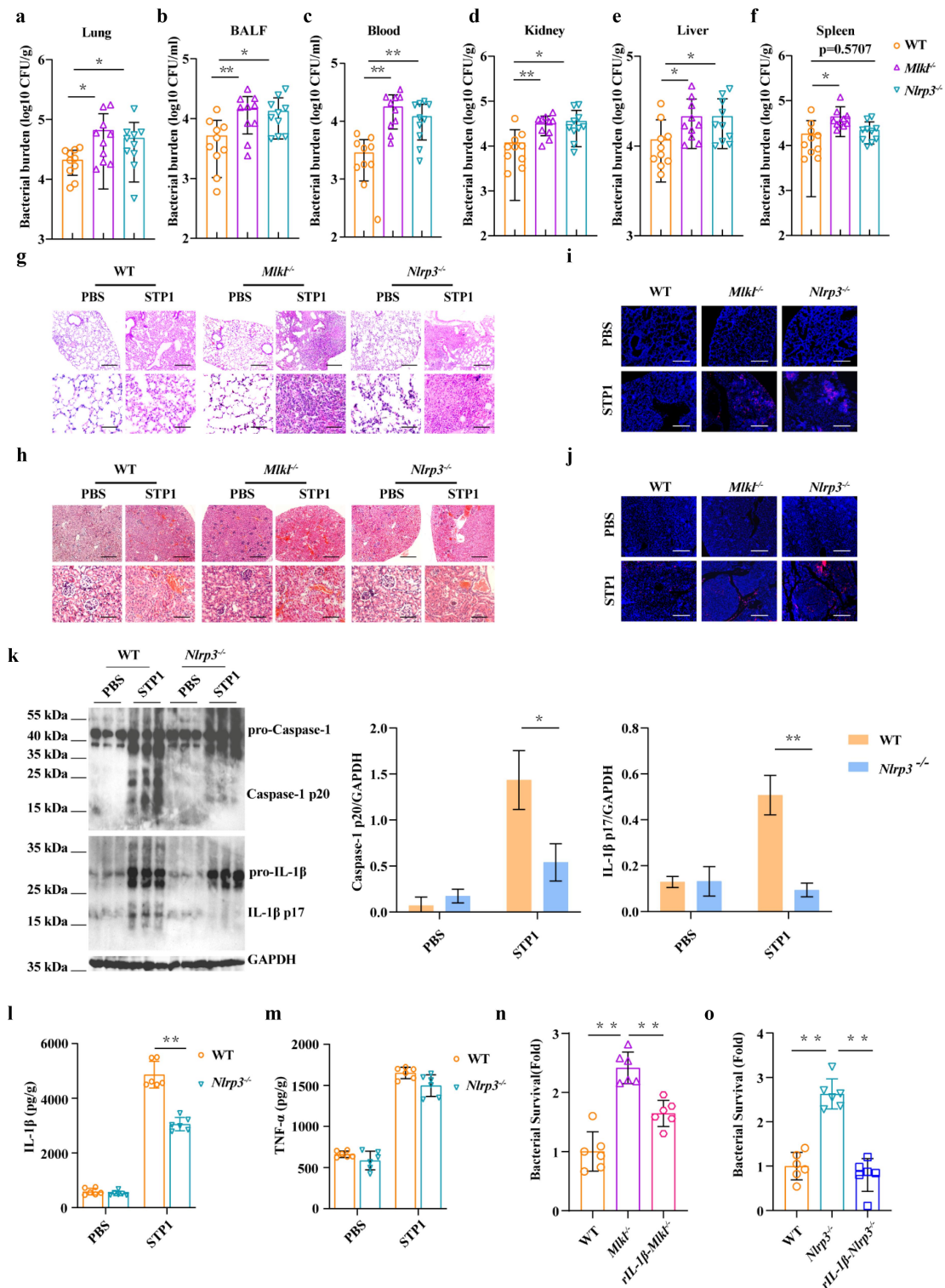


**Figure 5.** *Nlrp3* deficiency impairs bacterial clearance and is detrimental to the host protection. Age- and sex-matched WT, *Mikl*<sup>-/-</sup> and *Nlrp3*<sup>-/-</sup> mice ( $n = 10$ ) were inoculated intranasally ( $1 \times 10^9$  CFUs) or *i.v.* ( $1 \times 10^8$  CFUs) with *S. pluranimalium* strain STP1 for 24 h. (A-F) bacterial burden in the lung, BALF, blood, kidney, liver and spleen were quantitated. (G, H) representative lung and kidney tissue structures were observed by H&E staining (upper panel, magnification  $\times 100$ , lower panel, magnification,  $\times 400$ ). (I, J) representative TUNEL staining of apoptotic cells in the lung and kidney tissue (magnification,  $\times 400$ ). (K) lung tissues were collected, homogenized, and then immunoblotting for Caspase-1, IL-1 $\beta$  and GAPDH. Left, representative images of immunoblotting for Caspase-1 and IL-1 $\beta$  in lung tissues of WT and *Nlrp3*<sup>-/-</sup> mic. Right, amounts of Caspase-1 and IL-1 $\beta$  determined by densitometry of protein bands from three experiments. The GAPDH served as a loading control. (L, M) levels of IL-1 $\beta$  and TNF- $\alpha$  in lung were determined. LPS-primed WT, *Mikl*<sup>-/-</sup> and *Nlrp3*<sup>-/-</sup> BMDMs were incubated with rIL-1 $\beta$  (1000 pg/ml) or PBS for 1 h before challenged with *S. pluranimalium* strain STP1 (MOI = 25, 6 h). (N, O) the supernatants were collected and plated on TSB agar plates to enumerate the bacteria. Graphs are means  $\pm$  SD from data pooled 10 (A-F) or six (L-O) biological replicates. Statistical significance is indicated by \* $p < 0.05$ , \*\* $p < 0.01$ .

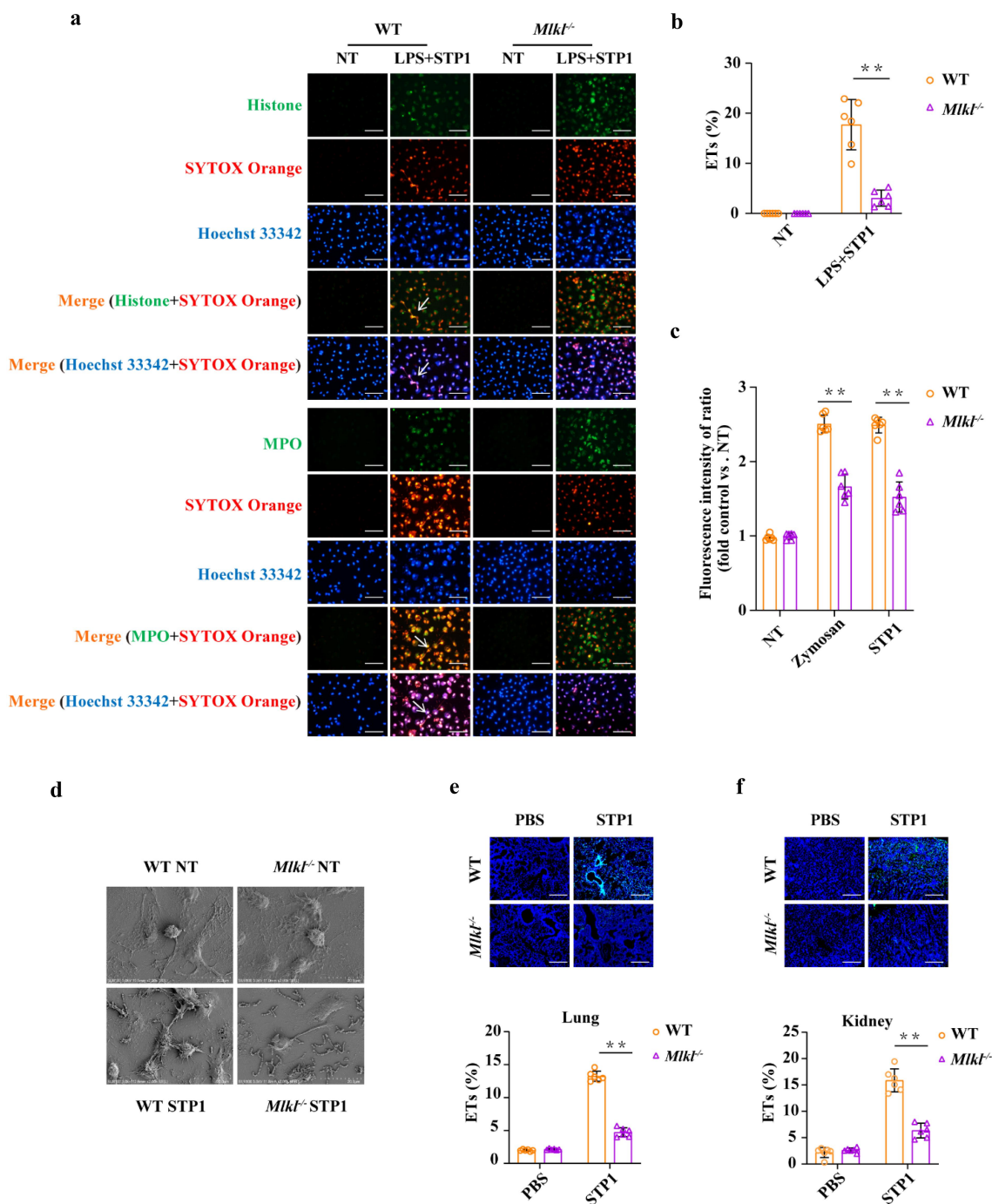


**Figure 6.** *Mikl* deficiency causes a reduction of *S. pluranimalium*-triggered extracellular trap formation. LPS-primed WT and *Mikl*<sup>-/-</sup> BMDMs were stimulated with *S. pluranimalium* strain STP1 (MOI = 25, 100 min). (A) representative immunofluorescence staining of METs formation as indicated by DNA decorated with histone or MPO within the ETs structures. Histone (green), MPO (green) and DNA (orange/blue). magnification,  $\times 400$ . (B) METs were quantified by Fiji and presented as the percentage of ETs. (C) quantification of bacteria-induced METs formation using SYTOX green. Zymosan (1 mg/ml) stimulated cells were used as positive control. (D) the METs release was detected by SEM. Age- and sex-matched WT and *Mikl*<sup>-/-</sup> mice were infected intranasally ( $1 \times 10^9$  CFUs) or *i.v.* ( $1 \times 10^8$  CFUs) with *S. pluranimalium* strain STP1 for 24 h. (E, F) representative immunofluorescence staining of histone was performed in lung and kidney sections, and ETs were quantified by Fiji and presented as the percentage of ETs. Graphs are means  $\pm$  SD from data pooled six (B, C, E and F) biological replicates. Statistical significance is indicated by \* $p < 0.05$ , \*\* $p < 0.01$ .



[35]. Although there is evidence that *S. pluranimalium* is sensitive to chloramphenicol, amikacin, enrofloxacin, and ciprofloxacin, it is also resistant to azithromycin, erythromycin, florfenicol, gentamicin, amoxicillin and sulfamonomethoxine [10]. With antibiotic resistance becoming a growing concern, the development of new preventive and therapeutic strategies has become very urgent. Since the ultimate outcome of an infectious process depends on the host-pathogen interaction and the host innate immune system provides the first line of defence against pathogen invasion, research on the innate immune response to *S. pluranimalium* is critical for design of potential therapeutic interventions.

*S. pluranimalium* has been reported as one of causative agents for respiratory disease, as well as a rare case of bacteraemia was reported [36,37]. Using murine *S. pluranimalium* pneumonia (intranasal inoculation) and systemic infection (intravenous inoculation) models, we demonstrated that MLKL contributes to host protection against *S. pluranimalium* pulmonary and systemic infection. In *S. pluranimalium* pneumonia model, *Mkl* deficiency results in increased mortality, more bacteria burden in BALF and lungs, severe destruction of lung architecture, and elevated inflammatory cells infiltration and inflammatory cytokines production. Correspondingly, compared with WT mice, *Mkl*<sup>-/-</sup> mice also showed elevated levels of bacteria in blood and various tissues, severe kidney injury and massive PMNs accumulation in the kidney following *S. pluranimalium* systemic infection. Therefore, we defined a novel role for MLKL in the host defence against *S. pluranimalium* infection. Currently, increasing evidence shows that inflammasomes are adequate for protecting the host against invasion and infection by gram-positive and gram-negative bacteria, viruses, fungi, parasites, and other pathogens [38–41]. Therefore, inflammasome signalling was evaluated to investigate the potential mechanisms of MLKL-mediated host protection. *Mkl* deficiency results in impaired inflammasome activation in the lung tissues following *S. pluranimalium* infection. Next, we investigated whether inflammasome signalling downstream of MLKL confers host protection against *S. pluranimalium* infection. Interestingly, supplementation with exogenous rIL-1 $\beta$  led to a dramatic reduction in the bacterial load and significantly alleviated pathological damage in the lung and kidney sections of *Mkl*<sup>-/-</sup> mice, suggesting that exogenous rIL-1 $\beta$  could reverse the susceptibility of *Mkl*<sup>-/-</sup> mice to *S. pluranimalium* infection. Hence, it is well-established that MLKL facilitates *S. pluranimalium* control by enhancing inflammasome activation.

Subsequently, we explored the molecular signalling mechanisms underlying MLKL-mediated host protection. Because p-MLKL is mainly located in recruited inflammatory cells, BMDMs were used in in vitro experiments to further investigate MLKL-mediated inflammatory responses upon infection with the pathogen *S. pluranimalium*. Notably, Consistent with the *in vivo* results, *Mkl* deficiency inhibited *S. pluranimalium*-triggered inflammasome signalling. Previous studies have shown that MLKL is an endogenous activator of the NLRP3 inflammasome, and active MLKL triggers the NLRP3 inflammasome in a cell-intrinsic manner, providing a mechanism for the concurrent processing and release of IL-1 $\beta$  [42,43]. Moreover, infection with certain pathogens can induce NLRP3 inflammasome assembly in human macrophages [44,45]. Therefore, we analysed whether MLKL-driven inflammasome activation is dependent on NLRP3 signalling. As expected, MLKL-driven inflammasome activation was notably inhibited in *Nlrp3*<sup>-/-</sup> BMDMs compared to their WT counterparts. It is well accepted that three mechanisms, potassium efflux [46], reactive oxygen species (ROS) generation [47] and lysosomal destabilization [48] activate the NLRP3 inflammasome. Furthermore, the minimal membrane permeabilization events associated with NLRP3 activation are potassium efflux and sodium influx [49]. We further found that *S. pluranimalium* elicits NLRP3 inflammasome activation in a potassium efflux-dependent manner. Moreover, we observed similar defects in host defence between *Mkl*<sup>-/-</sup> mice and *Nlrp3*<sup>-/-</sup> mice, as revealed by significantly increased bacterial loads, severe lung and kidney injury, and impaired inflammasome activation, substantiating that NLRP3 inflammasome signalling mediates MLKL's effect of MLKL on host defence. Furthermore, the administration of exogenous rIL-1 $\beta$  reversed the effects of *Mkl*<sup>-/-</sup> and *Nlrp3*<sup>-/-</sup> BMDMs in limiting the proliferation of *S. pluranimalium*. In conclusion, our results revealed that NLRP3 inflammasome signalling is implicated in the active MLKL-mediated host defence against *S. pluranimalium* infection.

Extracellular trap were reported to be a means by which innate immune cells such as neutrophils [50], macrophages [51], basophils [52], eosinophils [53], and mast cells [54] kill invading pathogens. The extracellular trap is released when the cells are exposed to a range of pathogenic and pro-inflammatory stimuli and consists of the backbone of DNA and histones, which are decorated with a range of other proteins [55]. It has been shown that these structures can capture, neutralize and kill different kinds of microbes, including viruses, bacteria, fungi and parasites [50]. Because of the defect in pathogen control in the absence of *Mkl*, we hypothesized that

MLKL is involved in the regulation of extracellular trap-dependent bactericidal mechanisms. As expected, defects in extracellular trap formation and extracellular DNA release were observed in *Mlkl*<sup>-/-</sup> macrophages. In line with *in vitro* results, *Mlkl* deficiency impaired extracellular trap formation in lung and kidney tissues of *S. pluranimalium*-infected mice, suggesting that the protective effect of MLKL against *S. pluranimalium* infection may also depend on ETs-mediated pathogen control. Meanwhile, active MLKL promotes extracellular trap formation release for the control of methicillin-resistant *Staphylococcus aureus* (MRSA) infection [56]. Recently, inflammasome signalling activation primes NETosis [57], in turn, enhanced formation of extracellular trap formation can lead to increase inflammasome-mediated pyroptosis [58]. In line with these, our previous study demonstrated that MLKL protects against *Clostridium perfringens* infection by enhancing NLRP3 inflammasome-extracellular traps axis [59]. Here, we provided a certain clue that MLKL contributes to host defence against *S. pluranimalium* infection by mediating NLRP3 inflammasome activation and extracellular trap formation. Additional evidence has shown that NLRP3 inflammasome activation and NETosis could be triggered simultaneously [60]. Based our results and other report, investigating the relationship between MLKL-driven NLRP3 inflammasome signalling and MLKL-mediated extracellular trap formation in host defence against *S. pluranimalium* infection will be promising and exciting.

In conclusion, the present study demonstrated that MLKL is required for host defence against *S. pluranimalium* infection *in vivo*. MLKL promotes pathogen control and inflammasome signalling activation. Notably, our results provide evidence that potassium efflux-dependent NLRP3 inflammasome activation, downstream of MLKL, facilitates bacterial eradication. Moreover, MLKL enhanced ETs formation, a powerful bactericidal mechanism in the innate immune defence, suggesting that ETs release is also involved in MLKL-mediated host defence. These observations document a novel biological role of MLKL in regulating innate immunity and provide clues regarding host-pathogen interactions.

### Supporting information

Identification and 16S rDNA sequencing analysis of the *S. pluranimalium* clinical isolate STP1 related to Figure 1 (Figure S1). Exogenous rIL-1 $\beta$  administration protected *Mlkl*<sup>±</sup>/*Nlrp3*<sup>±</sup> mice against *S. pluranimalium* infection, related to Figure 5 (Figure S2).

### Acknowledgements

The authors thank Prof. Yong-Jun Yang (Jilin University, China) for his kind assistance and guidance.

### Disclosure statement

No potential conflict of interest was reported by the author(s).

### Funding

This work was supported by the National Natural Science Foundation of China [No. 32302886, No. 32160832], Program for Young Talents of Science and Technology in Universities of Inner Mongolia Autonomous Region of China [No. NJYT22104], Research Program of Science and Technology at Universities of Inner Mongolia Autonomous Region of China [No. NJZZ21001], Natural Science Foundation of Inner Mongolia Autonomous Region of China [No. 2021BS03003], Student Innovation and Entrepreneurship Training Programs of Inner Mongolia University [No. 21400-23269204], Inner Mongolia University Startup Foundation for Advanced Talents [No. 30500-5185139], and Inner Mongolia Engineering Technology Research Center of Germplasm Resources Conservation and Utilization [No. 21400-222526].

### Data Availability statement

The data supporting the findings of this study are available from the corresponding author upon reasonable request.

### ORCID

Lin Yuan  <http://orcid.org/0009-0005-7390-8655>

Shui-Xing Yu  <http://orcid.org/0009-0007-1134-1715>

### References

- [1] Devriese LA, Vandamme P, Collins MD, et al. *Streptococcus pluranimalium* sp. nov., from cattle and other animals. *Int. J Syst Bacteriol.* 1999;49(3):t31221-1226. doi: 10.1099/00207713-49-3-1221
- [2] Fu DJ, Ramachandran A, Miller C. Miller C *Streptococcus pluranimalium* meningoencephalitis in a horse. *Journal of veterinary diagnostic investigation: official publication of the American Association of veterinary Laboratory Diagnosticians.* J Vet Diagn Invest. 2021;33(5):956-960. doi: 10.1177/104063872111023465
- [3] Hedegaard L, Christensen H, Chadfield MS, et al. Association of *Streptococcus pluranimalium* with valvular endocarditis and septicaemia in adult broiler parents. *Avian Patholo.* 2009;38(2):155-160. doi: 10.1080/03079450902737763
- [4] Pan Y, An H, Fu T, et al. Characterization of *Streptococcus pluranimalium* from a cattle with mastitis by whole genome sequencing and functional

- validation. *BMC Microbiol.* 2018;18(1):182. doi: [10.1186/s12866-018-1327-0](https://doi.org/10.1186/s12866-018-1327-0)
- [5] Foster G, Barley J, Howie F, et al. Streptococcus pluranimalium in bovine reproductive disease. *Vet Rec.* 2008;163(21):638. doi: [10.1136/vr.163.21.638](https://doi.org/10.1136/vr.163.21.638)
- [6] Aryasinghe L, Sabbar S, Kazim Y, et al. Streptococcus pluranimalium: a novel human pathogen? *Int J Surg Case Rep.* 2014;5(12):1242–1246. doi: [10.1016/j.ijscr.2014.11.029](https://doi.org/10.1016/j.ijscr.2014.11.029)
- [7] Duriseti P, Fleisher J. Streptococcus pluranimalium infective endocarditis and brain abscess. *IDCases.* 2019;18(e00587): doi: [10.1016/j.idcr.2019.e00587](https://doi.org/10.1016/j.idcr.2019.e00587)
- [8] Maher G, Beniwal M, Bahubali V, et al. Streptococcus pluranimalium: emerging animal streptococcal species as causative agent of human brain abscess. *World Neurosurg.* 2018;115:115208–115212. doi: [10.1016/j.wneu.2018.04.099](https://doi.org/10.1016/j.wneu.2018.04.099)
- [9] George K, Jacob G, B JS, et al. Pneumonia with synpneumonic effusion and bacteraemia: streptococcus pluranimalium infection in a healthy adult. *Br J Hosp Med.* 2020;81(2):1–3. (London, England: 2005). doi: [10.12968/hmed.2019.0275](https://doi.org/10.12968/hmed.2019.0275)
- [10] Ghazvini K, Karbalaee M, Kianifar H, et al. The first report of Streptococcus pluranimalium infection from Iran: a case report and literature review. *Clin Case Rep.* 2019;7(10):1858–1862. doi: [10.1002/ccr3.2374](https://doi.org/10.1002/ccr3.2374)
- [11] Zindel J, Kubes P. Damps, PAMPs, and LAMPs in immunity and sterile inflammation. *Annu Rev Pathol Mech Dis.* 2020;15(1):15493–15518. doi: [10.1146/annurev-pathmechdis-012419-032847](https://doi.org/10.1146/annurev-pathmechdis-012419-032847)
- [12] De Lorenzo G, Ferrari S, Cervone F, et al. Extracellular DAMPs in plants and mammals: immunity, tissue damage and repair. *Trends Immunol.* 2018;39(11):937–950. doi: [10.1016/j.it.2018.09.006](https://doi.org/10.1016/j.it.2018.09.006)
- [13] Ohto U. Activation and regulation mechanisms of NOD-like receptors based on structural biology. *Front Immunol.* 2022;13: doi: [10.3389/fimmu.2022.953530](https://doi.org/10.3389/fimmu.2022.953530)
- [14] Unterholzner L. The interferon response to intracellular DNA: why so many receptors? *Immunobiology.* 2013;218(11):1312–1321. doi: [10.1016/j.imbio.2013.07.007](https://doi.org/10.1016/j.imbio.2013.07.007)
- [15] Majer O, Liu B, Barton GM. Nucleic acid-sensing TLRs: trafficking and regulation. *Curr Opin Immunol.* 2017;44:4426–4433. doi: [10.1016/j.coi.2016.10.003](https://doi.org/10.1016/j.coi.2016.10.003)
- [16] Rehwinkel J, Gack MU. RIG-I-like receptors: their regulation and roles in RNA sensing. *Nat Rev Immunol.* 2020;20(9):537–551. doi: [10.1038/s41577-020-0288-3](https://doi.org/10.1038/s41577-020-0288-3)
- [17] Mnich ME, van Dalen R, van Sorge NM. C-Type lectin receptors in host defense against bacterial pathogens. *Front Cell Infect Microbiol.* 2020;10309: doi: [10.3389/fcimb.2020.00309](https://doi.org/10.3389/fcimb.2020.00309)
- [18] Sun L, Wang H, Wang Z, et al. Mixed lineage kinase domain-like protein mediates necrosis signaling downstream of RIP3 kinase. *Cell.* 2012;148(1–2):213–227. doi: [10.1016/j.cell.2011.11.031](https://doi.org/10.1016/j.cell.2011.11.031)
- [19] Wu J, Huang Z, Ren J, et al. Mlkl knockout mice demonstrate the indispensable role of Mlkl in necroptosis. *Cell Res.* 2013;23(8):994–1006. doi: [10.1038/cr.2013.91](https://doi.org/10.1038/cr.2013.91)
- [20] Yu SX, Zhou FH, Chen W, et al. Decidual stromal cell necroptosis contributes to polyinosinic-polycytidylic acid-triggered abnormal murine pregnancy. *Front Immunol.* 2017;8916: doi: [10.3389/fimmu.2017.00916](https://doi.org/10.3389/fimmu.2017.00916)
- [21] Galluzzi L, Kepp O, Chan FK, et al. Necroptosis: mechanisms and relevance to disease. *Annu Rev Pathol.* 2017;12103–12130. doi: [10.1146/annurev-pathol-052016-100247](https://doi.org/10.1146/annurev-pathol-052016-100247)
- [22] Choi ME, Price DR, Rytter SW, et al. Necroptosis: a crucial pathogenic mediator of human disease. *JCI Insight.* 2019;4(15): doi: [10.1172/jci.insight.128834](https://doi.org/10.1172/jci.insight.128834)
- [23] Nogusa S, Thapa RJ, Dillon CP, et al. RIPK3 activates parallel pathways of MLKL-Driven necroptosis and FADD-Mediated apoptosis to protect against influenza A virus. *Cell Host Microbe.* 2016;20(1):13–24. doi: [10.1016/j.chom.2016.05.011](https://doi.org/10.1016/j.chom.2016.05.011)
- [24] Ashida H, Mimuro H, Ogawa M, et al. Cell death and infection: a double-edged sword for host and pathogen survival. *The J Cell Bio.* 2011;195(6):931–942. doi: [10.1083/jcb.201108081](https://doi.org/10.1083/jcb.201108081)
- [25] Liu Y, Xing LH, Li FX, et al. Mixed lineage kinase-like protein protects against Clostridium perfringens infection by enhancing NLRP3 inflammasome-extracellular traps axis. *I Sci.* 2022;25(10):105121. doi: [10.1016/j.isci.2022.105121](https://doi.org/10.1016/j.isci.2022.105121)
- [26] Zhou W, Yuan J. Necroptosis in health and diseases. *Semin Cell Dev Biol.* 2014;35:3514–3523. doi: [10.1016/j.semcdb.2014.07.013](https://doi.org/10.1016/j.semcdb.2014.07.013)
- [27] Yu SX, Chen W, Liu ZZ, et al. Non-hematopoietic MLKL protects against salmonella mucosal infection by enhancing inflammasome activation. *Front Immunol.* 2018;9119: doi: [10.3389/fimmu.2018.00119](https://doi.org/10.3389/fimmu.2018.00119)
- [28] Martens S, Bridelance J, Roelandt R, et al. MLKL in cancer: more than a necroptosis regulator. *Cell Death Diff.* 2021;28(6):1757–1772. doi: [10.1038/s41418-021-00785-0](https://doi.org/10.1038/s41418-021-00785-0)
- [29] Ying Z, Pan C, Shao T, et al. Mixed lineage kinase domain-like protein MLKL breaks down myelin following nerve injury. *Molecular Cell.* 2018;72(3):457–468.e455. doi: [10.1016/j.molcel.2018.09.011](https://doi.org/10.1016/j.molcel.2018.09.011)
- [30] Zhan C, Huang M, Yang X, et al. MLKL: functions beyond serving as the executioner of necroptosis. *Theranostics.* 2021;11(10):4759–4769. doi: [10.7150/thno.54072](https://doi.org/10.7150/thno.54072)
- [31] Huang H, Harris R, Yun H, et al. RIPK3 Activates MLKL-Driven Necroptosis and NLRP3 Inflammasome in Macrophages to Protect Against Streptococcus Pneumoniae. *Am J Respir Crit Care Med.* 2019;199:A5914.
- [32] Huang H-R, Cho SJ, Harris RM, et al. RIPK3 activates MLKL-mediated necroptosis and inflammasome signaling during Streptococcus infection. *Am J Respir Cell Mol Biol.* 2021;64(5):579–591. doi: [10.1165/rcmb.2020-0312OC](https://doi.org/10.1165/rcmb.2020-0312OC)
- [33] Gutierrez KD, Davis MA, Daniels BP, et al. MLKL activation triggers NLRP3-mediated processing and release of IL-1 $\beta$  independently of gasdermin-D. *J Immunol.* 2017;198(5):2156–2164. doi: [10.4049/jimmunol.1601757](https://doi.org/10.4049/jimmunol.1601757)
- [34] Conos SA, Chen KW, De Nardo D, et al. Active MLKL triggers the NLRP3 inflammasome in a cell-intrinsic manner. *Proc Nat Acad Sci.* 2017;114(6):E961–E969. doi: [10.1073/pnas.1613305114](https://doi.org/10.1073/pnas.1613305114)



- [35] Yan B, Guo Y, Wang J, et al. Identification and histopathological analysis of *Streptococcus pluranimalium* caused pneumonia in sheep. *J Biotech Res.* 2022;13:10–17.
- [36] Kalhor DH, Luo S, Xie X, et al. *Streptococcus pluranimalium* isolated from a canine respiratory case: identification and experimental infection in mice. *Pak Vet J.* 2015;35(3):388–390.
- [37] Duriseti P, Fleisher JJI. *Streptococcus pluranimalium* infective endocarditis and brain abscess. *IDCases.* 2019;18:e00587. doi: [10.1016/j.idcr.2019.e00587](https://doi.org/10.1016/j.idcr.2019.e00587)
- [38] Clare B. Inflammasome activation by *Salmonella*. *Curr Opin Microbiol.* 2021;6427–6432. doi: [10.1016/j.mib.2021.09.004](https://doi.org/10.1016/j.mib.2021.09.004)
- [39] Costa Franco MMS, Marim FM, Alves-Silva J, et al. AIM2 senses *Brucella abortus* DNA in dendritic cells to induce IL-1 $\beta$  secretion, pyroptosis and resistance to bacterial infection in mice. *Microbes And Infection.* 2019;21(2):85–93. doi: [10.1016/j.micinf.2018.09.001](https://doi.org/10.1016/j.micinf.2018.09.001)
- [40] Wegiel B, Larsen R, Gallo D, et al. Macrophages sense and kill bacteria through carbon monoxide-dependent inflammasome activation. *The J Clin Investig.* 2014;124(11):4926–4940. doi: [10.1172/jci72853](https://doi.org/10.1172/jci72853)
- [41] Naseer N, Egan MS, Reyes Ruiz VM, et al. Human NALP/NLRC4 and NLRP3 inflammasomes detect *salmonella* type III secretion system activities to restrict intracellular bacterial replication. *PLOS Pathogens.* 2022;18(1):e1009718. doi: [10.1371/journal.ppat.1009718](https://doi.org/10.1371/journal.ppat.1009718)
- [42] Conos SA, Chen KW, De Nardo D, et al. Active MLKL triggers the NLRP3 inflammasome in a cell-intrinsic manner. *Proc Natl Acad Sci USA.* 2017;114(6):E961–e969. doi: [10.1073/pnas.1613305114](https://doi.org/10.1073/pnas.1613305114)
- [43] Gutierrez KD, Davis MA, Daniels BP, et al. MLKL activation triggers NLRP3-mediated processing and release of IL-1 $\beta$  independently of gasdermin-D. *J Immunol.* 2017;198(5):2156–2164. (Baltimore, Md: 1950). doi: [10.4049/jimmunol.1601757](https://doi.org/10.4049/jimmunol.1601757)
- [44] Chambers ED, White A, Vang A, et al. Blockade of equilibrative nucleoside transporter 1/2 protects against *Pseudomonas aeruginosa*-induced acute lung injury and NLRP3 inflammasome activation. *FASEB J.* 2020;34(1):1516–1531. doi: [10.1096/fj.201902286R](https://doi.org/10.1096/fj.201902286R)
- [45] Deng Q, Wang Y, Zhang Y, et al. *Pseudomonas aeruginosa* triggers macrophage autophagy to escape intracellular killing by activation of the NLRP3 inflammasome. *Infect Immun.* 2016;84(1):56–66. doi: [10.1128/iai.00945-15](https://doi.org/10.1128/iai.00945-15)
- [46] Ferrari D, Pizzirani C, Adinolfi E, et al. The P2X7 receptor: a key player in IL-1 processing and release. *J Immunol.* 2006;176(7):3877–3883. (Baltimore, Md: 1950). doi: [10.4049/jimmunol.176.7.3877](https://doi.org/10.4049/jimmunol.176.7.3877)
- [47] Tschopp J, Schroder K. NLRP3 inflammasome activation: the convergence of multiple signalling pathways on ROS production? *Nature reviews. Immunology.* 2010;10(3):210–215. doi: [10.1038/nri2725](https://doi.org/10.1038/nri2725)
- [48] Hornung V, Bauernfeind F, Halle A, et al. Silica crystals and aluminum salts activate the NALP3 inflammasome through phagosomal destabilization. *Nat Immunol.* 2008;9(8):847–856. doi: [10.1038/ni.1631](https://doi.org/10.1038/ni.1631)
- [49] Muñoz-Planillo R, Kuffa P, Martínez-Colón G, et al. K<sup>+</sup> efflux is the common trigger of NLRP3 inflammasome activation by bacterial toxins and particulate matter. *Immunity.* 2013;38(6):1142–1153. doi: [10.1016/j.immuni.2013.05.016](https://doi.org/10.1016/j.immuni.2013.05.016)
- [50] Brinkmann V, Reichard U, Goosmann C, et al. Neutrophil extracellular traps kill bacteria. *Sci.* 2004;303(5663):1532–1535. doi: [10.1126/science.1092385](https://doi.org/10.1126/science.1092385)
- [51] Doster RS, Rogers LM, Gaddy JA, et al. Macrophage extracellular traps: a scoping review. *J Innate Immun.* 2018;10(1):3–13. doi: [10.1159/000480373](https://doi.org/10.1159/000480373)
- [52] Yousefi S, Morshed M, Amini P, et al. Basophils exhibit antibacterial activity through extracellular trap formation. *Allergy.* 2015;70(9):1184–1188. doi: [10.1111/all.12662](https://doi.org/10.1111/all.12662)
- [53] Yousefi S, Gold JA, Andina N, et al. Catapult-like release of mitochondrial DNA by eosinophils contributes to antibacterial defense. *Nature Med.* 2008;14(9):949–953. doi: [10.1038/nm.1855](https://doi.org/10.1038/nm.1855)
- [54] Elieh Ali Komi D, Kuebler WM. Significance of mast cell formed extracellular traps in microbial defense. *Clin Rev Allergy Immunol.* 2022;62(1):160–179. doi: [10.1007/s12016-021-08861-6](https://doi.org/10.1007/s12016-021-08861-6)
- [55] Rasmussen KH, Hawkins CL. Hawkins C L role of macrophage extracellular traps in innate immunity and inflammatory disease. *Biochem Soc Trans.* 2022;50(1):21–32. doi: [10.1042/bst20210962](https://doi.org/10.1042/bst20210962)
- [56] D’Cruz AA, Speir M, Bliss-Moreau M, et al. The pseudokinase MLKL activates PAD4-dependent NET formation in necroptotic neutrophils. *Sci Signaling.* 2018;11(546):eaao1716. doi: [10.1126/scisignal.aao1716](https://doi.org/10.1126/scisignal.aao1716)
- [57] Huang W, Jiao J, Liu J, et al. MFG-E8 accelerates wound healing in diabetes by regulating “NLRP3 inflammasome-neutrophil extracellular traps” axis. *Cell Death Discovery.* 2020;6(1):84. doi: [10.1038/s41420-020-00318-7](https://doi.org/10.1038/s41420-020-00318-7)
- [58] Cao Y, Shi M, Liu L, et al. Inhibition of neutrophil extracellular trap formation attenuates NLRP1-dependent neuronal pyroptosis via STING/IRE1 $\alpha$  pathway after traumatic brain injury in mice. *Front Immunol.* 2023;14:141125759. doi: [10.3389/fimmu.2023.1125759](https://doi.org/10.3389/fimmu.2023.1125759)
- [59] Liu Y, Xing L-H, Li F-X, et al. Mixed lineage kinase-like protein protects against *Clostridium perfringens* infection by enhancing NLRP3 inflammasome-extracellular traps axis. *i Sci.* 2022;25(10):105121. doi: [10.1016/j.isci.2022.105121](https://doi.org/10.1016/j.isci.2022.105121)
- [60] Singh P, Kumar N, Singh M, et al. Neutrophil extracellular traps and NLRP3 inflammasome: a disturbing duo in atherosclerosis. *Inflammation And Atherothrombosis.* 2023;11(2):261. doi: [10.3390/vaccines11020261](https://doi.org/10.3390/vaccines11020261)